DYNAMIC OPTIMIZATION OF MULTI-SPACECRAFT RELATIVE NAVIGATION CONFIGURATIONS IN THE EARTH-MOON SYSTEM

Benjamin Villac[*]**, Channing Chow**[†]**, Martin Lo**[‡]**, Gerald Hintz**[§]**, Zahra Nazari**[¶]

In this paper, the notion of relative navigation introduced by Hill, Lo and Born is analyzed for a large class of periodic orbits in the Earth-Moon three-body problem, due to its potential in supporting Moon exploration efforts. In particular, a navigation metric is introduced and used as a cost function to optimize over a class of periodic orbits. While the problem could be solve locally as an optimal control problem, a dynamical based approach that allows for a global/systematic view of the problem is proposed. First, the simpler problem of multiple spacecraft placement on a given periodic orbit is solved before the notion of continuation and bifurcation analysis is used to expand the range of solutions thus obtained.

INTRODUCTION

The Moon is a critical destination for the development of space. While it certainly is a stepping stone on the way to Mars, it is itself a world of wonder and resources as yet almost entirely unknown and unexplored. The vision we have is that one day soon, it will be a busy place of human activities. As such, infrastructures are needed to aim in the transport of both human and cargo between the Earth and the Moon. In particular, we envision a GPS-like system both in constellation around the Moon itself and in a cycler orbit between the Earth and the Moon. This could possibly be an extension of NASA's InterPlanetary Network (IPN) exploiting the low energy dynamics of the Interplanetary Superhighway between the Earth and the Moon. Such a telecommunications and navigation system should and could easily maintain itself autonomously with infrequent periodic checks on the ground to maintain its accuracy. Traffic between the Earth and the Moon would use the signals from the beacons to guide it to the Earth or the Moon. This paper explores the Multi-Spacecraft Relative Navigation of such a fleet of spacecraft in a cycler orbit between the Earth and the Moon.

This paper is based on the work on the LIAISON (Linked Autonomous Interplanetary Satellite Orbit Navigation) relative navigation in a series of papers by Hill, Lo, and Born. The basic idea is to exploit the asymmetry of the gravitational field to provide absolute position determination. We introduce a new navigation metric. This is used as a cost function to optimize over a class of cycler

---

[*]Assistant Professor; Mechanical and Aerospace Engineering, University of California, Irvine; bvillac@uci.edu; Tel: 949.824.8148.

[†]Graduate student; Astronautical Engineering, University of Southern California; channinc@usc.edu

[‡]Technologist; Jet Propulsion Laboratory, California Institute of Technology; Martin.W.Lo@jpl.nasa.gov

[§]Adjunct Professor; Astronautical Engineering, University of Southern California; ghintz@usc.edu

[¶]Graduate student; Mechanical and Aerospace Engineering, University of California, Irvine; znazari@uci.edu

periodic orbits. Our results are preliminary since the class of orbits explored so far is limited. In subsequent papers, we intend to further expand this work to a greater class of periodic orbits.

The paper begins with a review of the Circular Restricted 3-Body Problem followed by a study of several families of periodic orbit families using AUTO. LIAISON navigation is reviewed next. The α parameter from LAISON theory which measures the normalized sum of the absolute value of the range acceleration is introduced. Our new parameter, called $Var(\alpha)$, is the bounded variation of the time derivative of α integrated over one orbital period. This is novel main class optimization parameter for this paper. This is used to formulate a systematic approach to the dynamic optimization of multiple spacecraft relative navigation configurations. The down select process is in three stages: optimization over the class of periodic orbits, optimization over the configuration of the constellation, and optimization over the serviceability to end-users. The key metric for servicibility is GDOP (Geometric Dilution of Precision). The next section describes the optimization problems and results, followed by the conclusions.

DYNAMICAL MODELING

The motion of spacecrafts in the Earth-Moon system is strongly influenced by both the Earth and Moon gravity fields, but also by solar perturbations. In particular, the Sun's influence results in a time-varying dynamical system having no periodic orbits, but only quasi-periodic orbits. These orbits, however, are close enough from periodic orbits in the unperturbed model (i.e. without the influence of the Sun) that they can be obtained via differential correction from the simpler autonomous approximation to the motion.

While this approximation results in neglecting certain classes of orbits (such as the Sun-Earth libration orbits), it is a good approximation to start the analysis of mission concepts and allows us to use of the theory developed around the concept of periodic orbits to provide the detailed structure of the problem considered.

This section briefly reviews the main features of the well-known circular restricted 3-body problem (CR3BP) in order to establish the conventions used in this paper and the fundamental results about periodic orbits in autonomous, conservative systems that will be used in the reminder of the text.

Review of the CR3BP

Consider the circular restricted 3-body problem (CRTBP) with the two primary point masses m_1 (Earth) and m_2 (Moon) and the infinitesimal m_3 (spacecraft). The mass m_3 is assumed to be so small that it does not affect the motion of the primaries. The synodic reference frame is chosen with the x-axis directed from the Earth to the Moon and the y-axis orthogonal to the x-axis in the primary plane of motion. The z-axis is along the orbital angular momentum vector of the Earth and Moon and the units are normalized so the Earth-Moon distance is one unit and the period 2π time units. In this reference system, the gravitational parameter of the Moon is $\mu = 0.01215$ and that of the Earth is $1 - \mu$. The Earth is located at $x = -\mu$ while the Moon at $x = +1 - \mu$ as illustrated in Figure 1. This figure also indicates the location of the five equilibrium points, or libration points, where gravitational and centrifugal forces balance each other in this model (expressed in the synodic frame).
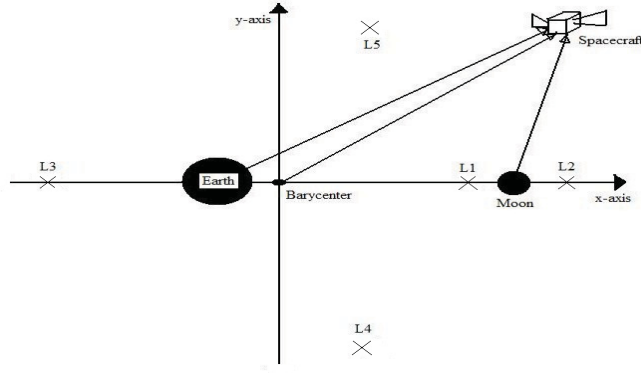
Figure 1: CR3BP reference frame.

The equations of motion (EOM) of m_3 for the non-dimensionalized CR3BP[1,2] are

$$\ddot{x} - 2\dot{y} = \frac{\partial U}{\partial x} = x - (1 - \mu)\frac{x + \mu}{r_1^3} - \mu\frac{x + \mu - 1}{r_2^3} \tag{1}$$

$$\ddot{y} + 2\dot{x} = \frac{\partial U}{\partial y} = \left(1 - \frac{1 - \mu}{r_1^3} - \frac{\mu}{r_2^3}\right)y \tag{2}$$

$$\ddot{z} = \frac{\partial U}{\partial z} = \left(\frac{\mu - 1}{r_1^3} - \frac{\mu}{r_2^3}\right)z \tag{3}$$

where

$$U = \frac{1}{2}\left(x^2 + y^2\right) + \frac{1 - \mu}{r_1} + \frac{\mu}{r_2}, \tag{4}$$

$$r_1 = \sqrt{(x + \mu)^2 + y^2 + z^2}, \qquad r_2 = \sqrt{(x - 1 + \mu)^2 + y^2 + z^2} \tag{5}$$

with $\mu = m_2$ and $1 - \mu = m_1$, and the range magnitudes r_1 and r_2 defined as the distances of spacecraft from the Earth and the Moon, respectively.

We note the autonomous (time-independent) nature of the system, which allows us to choose the phase of a spacecraft on an orbit for any epoch, as will be done in the optimization problem formulation.

Periodic orbits and constellations

One of the advantage of using the CR3BP as our base model, is the availability of periodic orbits, for which many results are known. In particular, these orbits can be organized into families which locally form smooth surfaces in phase space called invariant manifolds. The manifolds govern the flow of nearby trajectories. These families can, moreover, be succinctly represented by their characteristics, as illustrated in Figure 2 for the well-known families around the $LL1$ point, and be easily computed via numerical continuation methods,[3] such as pseudo-arc length or Poincare

3

section based methods. In this study, the software AUTO2000[4] has been used to perform these computations.
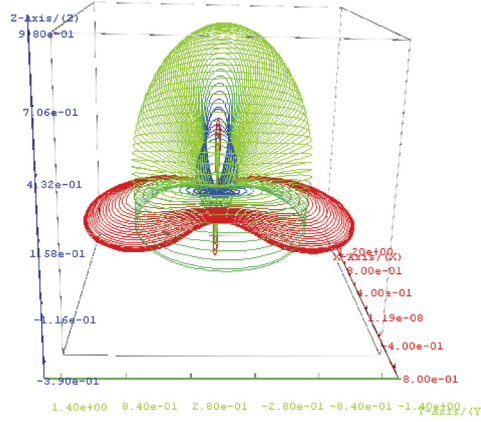

Figure 2: Sample periodic orbits families. (Left) planar and vertical Lyapunov families associated with the LL1 point. (Right) Characteristics.

Given that a spacecraft will repeat its path periodically, the placement of several spacecrafts on such an orbit constitutes a constellation. In particular, with minimal station-keeping effort, the constellation will maintain its properties over time. The viewpoint taken in this paper is one of optimizing constellation designs over the set of periodic orbits.

Structure of Periodic orbit families Besides the notion of family (or branch) of a periodic orbit as a (locally) smooth one-parametric set of orbits, the notion of bifurcation allows us to organize the different families together. In particular, two distinct families intersecting in the space of orbits are said to bifurcate from each other. The intersecting orbit is referred to as a branch point or bifurcating orbit. Numerical continuation allows for the detection of bifurcating orbits along a family and allows for branch switching, that is the exploration of new solution from known ones. The systematic procedure of continuation, bifurcation detection, branch switching and continuation of the new branches enables to theoretically represent the set of periodic orbits and provides an algorithmic scheme to compute any periodic orbit.

Starting from the linearized dynamics around the Libration points, one is thus able to generate a bifurcation diagram (i.e. the compilation of all the periodic orbits families characteristics) that succinctly represent a large set of orbits. This is illustrate in Figure 3. Each periodic orbit is thus represent by a single point in this graph; the x-axis corresponds to the averages of the x-coordinate along the orbits ($\int x(t)dt$) while the z-axis represent the maximum (or minimum) z-coordinate reached over an orbit.

4
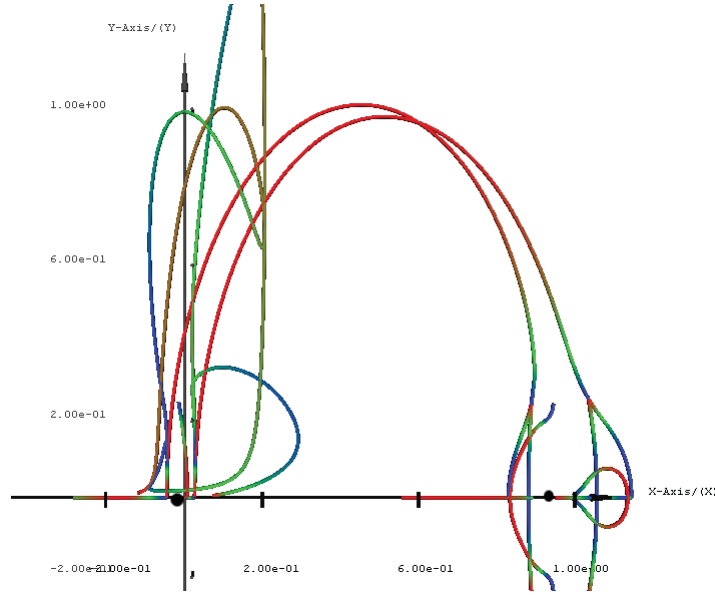
Figure 3: Bifurcation for the CR3BP, starting from the LL1 and LL2 points. The color along each branch corresponds to the period of the orbit, blue representing a shorter period and red a larger period. The black dots represent the location of the Earth and Moon.

Periodic constellation While the notion of constellation is not restricted to periodic motion, it is associated with bounded variations in time of the relative configurations between the spacecrafts. Placing a sequence of spacecrafts on a single periodic orbits offers the simplest possible constellation with periodic variations in time. This restricted class of constellations is still large and the study of the present paper. Figure 2 illustrate this concept.

In particular, the design of such constellations involve the choice of the number of spacecrafts, their placement and control. In our case, note that the autonomous nature of the dynamics implies that the constellation of N spacecrafts is determined by $N-1$ phases. Indeed, letting X_{10} denote the state of the first spacecraft at time t_0, its state on any other point on the orbit can be expressed $X_1(t) = \phi(t, t_0, X_{10})$, where the function ϕ denotes the flow of the dynamics. The state of the ith spacecraft at time t_0 can then be expressed as $X_i = \phi(\tau_i, t_o, X_{10})$ while its state at time t is given as $X_i = \phi(\tau_i, t, X_1(t))$. Thus only the relative position at an initial epoch of the spacecrafts along the chosen periodic orbits matter and the first spacecraft can be assumed to be on the $x - axis$ at time t_0, for example.

The initial placements of the spacecraft on a given periodic orbits is thus reduced to a finite dimension optimization problem on the time shifts τ_i (or phases $\frac{2\pi/T}{\tau}_i$), with a relevant metric for the application chosen. Note that while the metric should thus reduce to a function on the initial state of the spacecraft, it should be invariant with respect to first spacecraft position and should thus be an average over an orbit.

RELATIVE NAVIGATION CONSTELLATIONS

Relative navigation can be thought of in two ways: (1) with respect to the spacecrafts within the constellation, and (2) from the perspective of an end-user. This paper will address both interpreta-

tions as they pertain to optimization strategies.

From the first interpretation, the notion of relative, autonomous navigation, as introduced by Hill and Born,[1] builds on the concept that the orbit determination (OD) problem is solvable between spacecraft of a particular constellation without supplemental input from the ground. The idea focuses on using only satellite-to-satellite tracking (SST) to estimate the states for all of the participating spacecraft simultaneously. This new method is aptly termed linked, autonomous, interplanetary satellite orbit navigation (LIAISON), hereafter used synonymously with the word *liaison* in lieu of the explicit acronym. While other strategies could be used in conjunction with (or in place of) liaison navigation, this method provides a representative method to develop a framework for autonomous navigation constellation optimization.

In the second interpretation, the basic idea reflects the ancient paradigm of maritime navigation whereby the nighttime stars were used for guidance and course design. Analogous in astronautics, orbit determination knowledge is attained by an end-user (the receiver) using the spacecrafts within an existing constellation (transmitters) as guideposts. The most notable contemporary example of such a scheme is the global positioning system (GPS). Fortunately, since GPS accuracy metrics are mathematically generic, several GPS-like precision factors can be used synonymously with any navigation constellation without loss of generality.

Liaison Navigation Overview

Liaison navigation is predicated upon an axiom of uniqueness. If there exists an orbit that is unique, then its absolute orientation is spatially unambiguous, and therefore any other orbit measured with respect to that orbit will, likewise, also be unambiguous.

Building on this assertion, satellites that are in orbits which have sufficiently distinguishable characteristics, are most attractive for this type of navigation. Fortunately for spacecraft orbiting in the Earth-Moon neighborhood, this dynamic three-body environment provides the appropriate conditions for unique trajectories. Natural candidates for this study are periodic and quasi-periodic orbits.

A tandem goal in configuring liaison navigation constellations consists of reducing the numerics such that the spacecrafts can perform their own OD processing without any aid from the ground. As a direct consequence of the solvability of the OD problem in the asymmetric environment of the Earth-Moon system, the required OD inputs are reduced to mere scalar measurements of range. Radiometric observations can now consist solely of crosslink range and/or integrated Doppler data.

This method of intersatellite communication shows that it is possible to achieve a mutual understanding of orbital states, independently from third-party involvement. The authors not only demonstrated the feasibility of this novel OD technique, but also its potential to be a highly accurate means of navigation.

In exploring the circumstances that make liaison navigation viable, several constellation design principles and guidelines are developed.

First, it is apparent that by exploiting the asymmetries of the acceleration field, the necessary conditions for uniqueness are achieved. From this realization it becomes convenient to define a metric with which to quantitatively gauge the strength of the asymmetry in a system. The α parameter is introduced as a measure for comparing a single perturbing acceleration with respect to the sum of

all inertial accelerations [*]

$$\alpha_j(x, y, z) = \frac{|\ddot{\boldsymbol{r}}_j(x, y, z)|}{\sum_{i=1}^{n} |\ddot{\boldsymbol{r}}_i(x, y, z)|} \tag{6}$$

where j is the particular perturbing acceleration out of n total accelerations, and α is implicitly a function of time. Plotting the α parameter for the third-body effect, due to the Moon (α_{Moon}), allows for straightforward visual identification of regions of high asymmetry (i.e. high α).
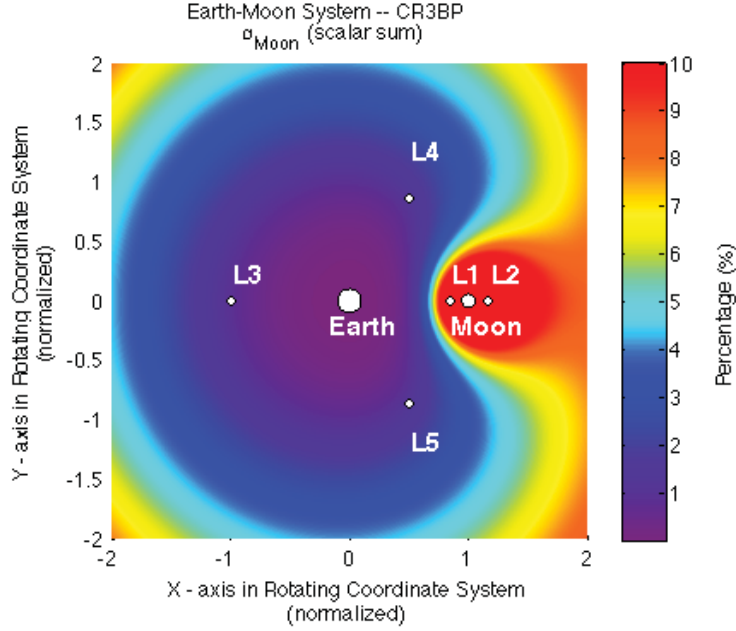
Figure 4: The α map showing the percentage of the Moon's acceleration with respect to the total acceleration of the system. The color gradient is truncated at **10%** to highlight the detail outside of the Moon's sphere of influence. The Earth is plotted at the origin, the Moon is at **1** on the x-axis, and the remaining five "white dots" are the lunar Lagrange points LL**1** - LL**5**.

A close-up of the area near the Moon's sphere of influence is shown to highlight the locations of the two lunar libration points (LL1 and LL2) with respect to the asymmetries of the system. The presence of these Lagrange points in the vicinity of high asymmetry further reinforces the selection of periodic and quasi-periodic orbits for liaison navigation.

Note that there exists one unavoidable symmetry. The north-south symmetry (above and below the plane of rotation of the primaries) originally suffers from an ambiguity in the sign of the z component. Although this prompts the use of the term "local-uniqueness", the generalization of "uniqueness" is usually kept since the resolution of this ambiguity can easily be handled with *a priori* information.

Building on the idea that α gauges asymmetry, a new parameter is developed to quantify the

---

[*]While the Earth-Moon system is often studied in a synodic reference frame, as illustrated in this paper, the data from the inertial measurement units on a spacecraft, however, allow for the estimation of the inertial accelerations rather than the synodic accelerations.
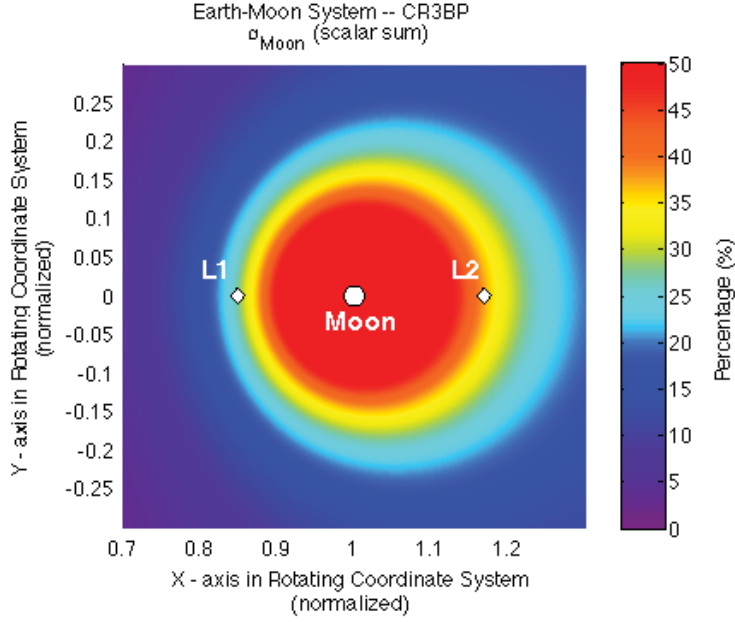
Figure 5: A zoomed-in view of the α map focusing on the region near the Moon's sphere of influence. The Moon is plotted at the origin and the lunar Lagrange points LL**1** and LL**2** are shown on either side, respectively.

"goodness" of the asymmetry experienced by an entire constellation. More precisely, the variations in α, that is the difference in α values between two points on an orbit, can be thought of as a measure of asymmetry. Additionally, by taking the limit of the difference in α values as a spacecraft moves along an orbit and averaging over an orbit, one obtains the bounded variation of the function $\alpha(t)$. In essence, orbits that span regions where large changes in α are experienced will tend to be better suited for relative navigation techniques. Therefore $Var(\alpha)$ can be considered a representative measure of asymmetry for the entire orbit.

$$Var(\alpha) = \int_0^T \left| \frac{\mathrm{d}\alpha}{\mathrm{d}t} \right| \, \mathrm{d}t \tag{7}$$

While $Var(\alpha)$ is used as a first-round indicator of potentially viable constellations, it gives little understanding of how the phasing of spacecrafts within a constellation affect the navigation accuracies of the system. At the moment, barring any physical limitations of a configuration, the spacing of the spacecraft should be such that relative navigation can achieve the most accurate estimations both for autonomy and for the end-user. In response, a statistical orbit determination approach is used to address this concern.

Batch processing allows for the propagation of the covariance matrix over the entire fit span of simulated data. This analysis provides a useful metric to indicate the accuracy of the orbit estimates.

$$\beta = 3 \max \left(\sqrt{\lambda} \right) \tag{8}$$

The β parameter, by definition, is set to be three times the square-root of the largest eigenvalue, λ_j, of the covariance matrix. In effect, this gives a conservative estimate on the overall size of the error in the solution (analogous to selecting the largest dimension of an ellipsoid to represent a sphere). Because the β parameter derives from a common statistical error measure, its application is not limited to certain orbital configurations and therefore may be applied generically. An in-depth development of this parameter can be found in the appendix.

End-User Navigation Overview

In many respects, spacecraft end-user navigation is functionally equivalent to a terrestrial user using GPS satellites for point-positioning. The core foundation is based on calculating the unknown position of a receiver with respect to several known and disparately placed transmitters. In effect, this type of orbit determination is an abstraction of the familiar geometric process of triangulation.

Though, in principle, the position of an observer can be determined using any subset of four spacecraft, the quality of the measurement is not the same for each combination. As it turns out, the driving force behind the quality of orbital estimation is the geometric placement of the spacecrafts with respect to the observer. In other words, it matters which four points are chosen to determine an orbit.

To quantify the effect of spatial orientation on estimation accuracy, the standard dilution of precision (DOP) factors are used. Out of the five customary definitions, the one parameter of interest is the geometric dilution of precision (GDOP).

$$\text{GDOP} = \sqrt{\sigma_1^2 + \sigma_2^2 + \sigma_3^2 + \sigma_4^2} \tag{9}$$

where the σ's are the standard deviations and the subscripts $1, 2, 3, 4$, refer to the four components of the unknown state vector (typically three rectangular coordinates and an associated receiver error term). The GDOP parameter scales inversely proportional to the quality of the geometric placement of the spacecrafts, namely smaller GDOP values indicate better orientations.

Optimization Metrics Overview

Several optimization metrics will be developed, each with application to a different phase of the optimization strategy. In particular, a total of three parameters will be discussed. The novel class optimization parameter, $Var(\alpha)$, will be the main focus of this section, with the other two parameters given only brief treatments saving any extensive formulations for the appendices.

Recall, the goal is to formulate a systematic approach to the dynamic optimization of multi-spacecraft relative navigation configurations. As such, little emphasis will be put on *a priori* knowledge for orbit selection, in favor of allowing the mathematics to reduce the solution space dynamically. The down-select process can be categorized into three stages: (1) optimization over the class of periodic orbits, (2) optimization over the configuration of a constellation, and (3) optimization over serviceability to end-users. Although it is envisioned that the problem should be addressed in the above sequence, in principle, this need not be true.

At the onset of the systematic optimization study, a functional is required to cull out inviable constellations within large classes of orbits. To do this, it is important to identify a common property that is shared within a class. Conveniently, the α parameter provides the necessary quantity with which to characterize the orbits with respect to the underlying dynamics of the system.

If α, as defined in Eq.(6), is a function of position and time, a more useful metric is produced when evaluating the changes in α over the entire orbit. This can be viewed as measuring how α is expected to change over time. In theory, the change in α should roughly indicate how the orbit is situated with respect to the Earth-Moon acceleration environment. It is of particular interest that this change in α be large, such that the orbit has a higher likelihood of being near the vicinity of both primaries, thereby enabling better liaison navigation.

The bounded variation of the time rate of change of α integrated over one orbital period yields the $Var(\alpha)$ parameter given in Eq.(7). For the purposes of numerical routines, it is often desirable to represent the quadratures in discrete form.

$$Var(\alpha) = \lim_{n \to \infty} \frac{1}{n} \sum_{i=1}^{n} \left| \frac{\mathrm{d}\alpha}{\mathrm{d}t} \right|_i \tag{10}$$

where, in practice, there are n total ephemeris points in the fitting interval. A simple example is presented to illustrate the values of $Var(\alpha)$ as they pertain to a representative set of north-south oscillating halo orbits.

A sample set of 8 halo orbits are generated about the LL2 point in the synodic system. The $Var(\alpha)$ parameter is evaluated per orbit to demonstrate the ability of the variations of α to capture, in a single metric, the amount of asymmetry spanned by each orbit. Different vantage points are shown by varying the camera azimuth and elevation angles – view(az,el).

Line Color	Value
	0.5130
	0.1934
	0.1685
	0.1546
	0.1472
	0.1400
	0.1342
	0.1271
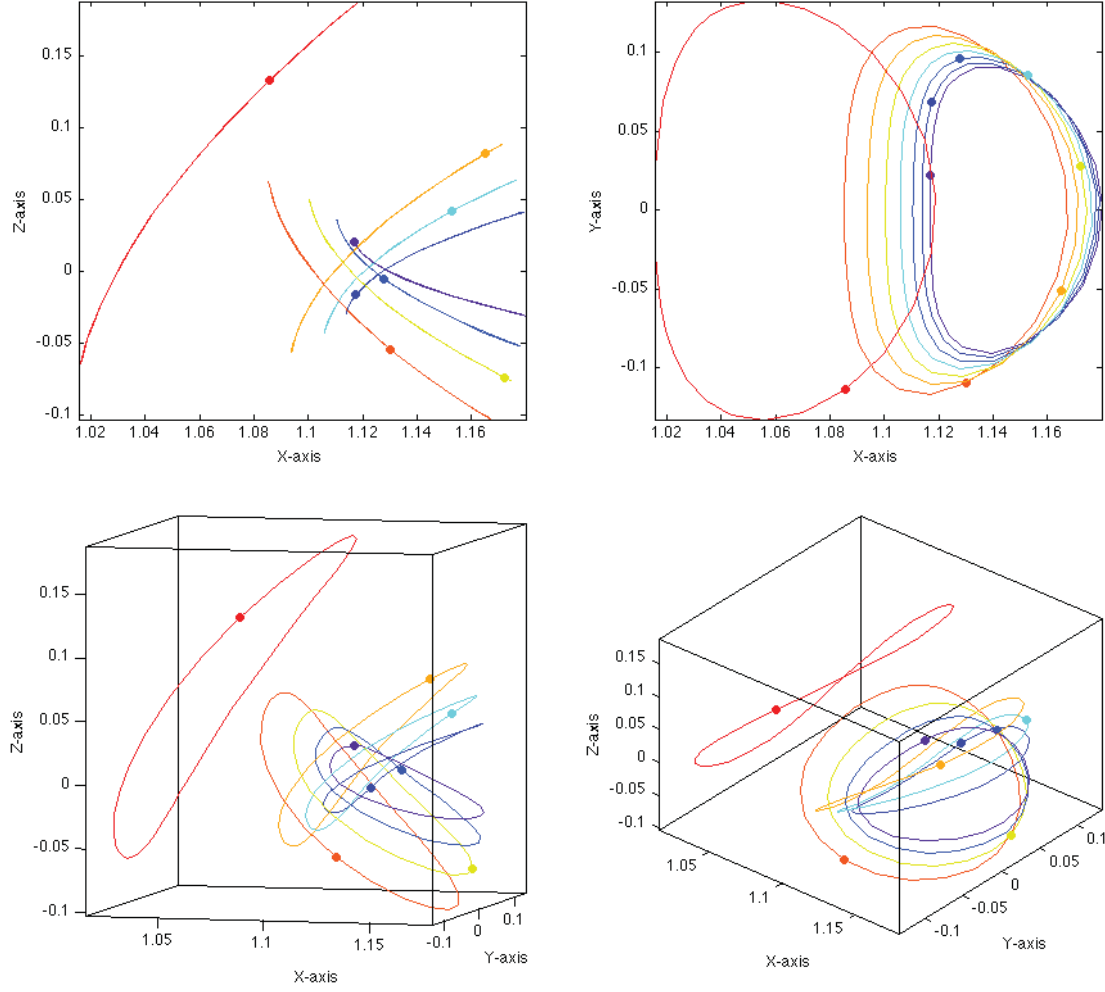
Figure 6: 8 halo orbits at LL2 – starting from the upper left corner and continuing clockwise, the views are (0,0), (0,90), (40,40), (15,5).

It is evident that the longest period halo orbit (represented as the red trajectory), which spatially occupies a larger region in the asymmetric environment, indeed achieves the largest $Var(\alpha)$ value. This novel parameter aids the optimization process in the capacity of numerically simulating the intuition of selecting the best liaison navigation candidates from entire classes of orbits, by weighing their interaction with the underlying dynamical system.

Once the class of periodic orbits has been whittled down to a few potential trajectories, the next optimization stage is primed for constellation configuration. Here, more traditional statistical orbit determination techniques are employed to find a measure of accuracy that captures the quality of spacecraft placements within the constellation.

The performance index is chosen to be the β parameter as defined by Eq.(8). In general, this metric indicates how well the state was estimated by means of quantifying the size of the error ellipsoid generated during the orbit determination process. The covariance matrices that contain

these standard deviations exist per time step and per constellation configuration. So, it becomes necessary to define a more conglomerate metric to gain a sense of navigation knowledge for an entire constellation for, say, one orbital period.

With the aid of the state transition matrix, β_i can be computed at any time within the observation interval. To gain an understanding of how the error behaves over the time span of interest, β_i may be averaged over the fitting interval as

$$\bar{\beta} = \frac{1}{n} \sum_{i=1}^{n} \beta_i \tag{11}$$

where there are n values of β_i in the fit span. For multiple spacecraft, the $\bar{\beta}$ of all pairwise combinations of the spacecrafts can be averaged to obtain a metric for the navigation knowledge accuracy for the constellation.

$$\beta_{\text{ave}} = \frac{1}{m} \sum_{k=1}^{m} \bar{\beta}_k \tag{12}$$

for m combinations of spacecrafts taken two at time (i.e. the binomial coefficient). Furthermore, since β_{ave} will vary with spacecraft spacing, it is specific to a particular orbital architecture. So, conducting a thorough survey of various geometries within a constellation will produce different β_{ave}, namely one per investigation. Selecting one representative β_{ave} with which to characterize a constellation as a whole (irrespective of specific spacecraft placements) can be achieved by

$$\beta_{\text{con}} = \min \begin{bmatrix} (\beta_{\text{ave}})_1 \\ (\beta_{\text{ave}})_2 \\ \vdots \\ (\beta_{\text{ave}})_p \end{bmatrix} \tag{13}$$

where p indicates the total number of configurations explored per constellation. Note, since there is theoretically an infinite number of spacecraft arrangements possible, this method of selecting the best β_{ave} from a finite set at discrete intervals, only serves as an approximation for that constellation.

The optimization metric, β_{con}, provides another useful functional for a thorough analysis of potential liaison constellations. Identifying optimal configurations for relative navigation can now be systematically evaluated with the information provided by this cost function.

Lastly, the optimal constellation should be able to provide accurate positioning service for an end-user. Stemming from a similar statistical analysis construct, the covariance matrix is once again utilized to generate error metrics. This inverse of the information matrix is produced during the kinematic positioning of an observer relative to several targets. With the GDOP figure of merit, as defined in Eq.(9), the accuracy of the solution can be computed per instance of a position determination. Again, in order to gauge the overall quality of the serviceable area of the proposed constellation, an integration of this GDOP metric is required over both time and space.

Considering that a constellation configuration is already chosen using the above optimization metrics, the quality of positioning in its serviceable area may be approximated by the following four dimensional integral

$$\text{GDOP}_{\text{con}} = \int_{\tau} \iiint_{V} (\text{GDOP}) \, d\tau \, dV \tag{14}$$

for one constellation orbital period τ and a volume of space V (theoretically limited only by instrument communications capability). Since the idea is to obtain a representative parameter for an entire constellation, all available spacecraft observations will be used in the GDOP computation (as opposed to only the minimum of four). This assumption also alleviates computational intensity when considering all combinations of spacecraft taken four at a time.
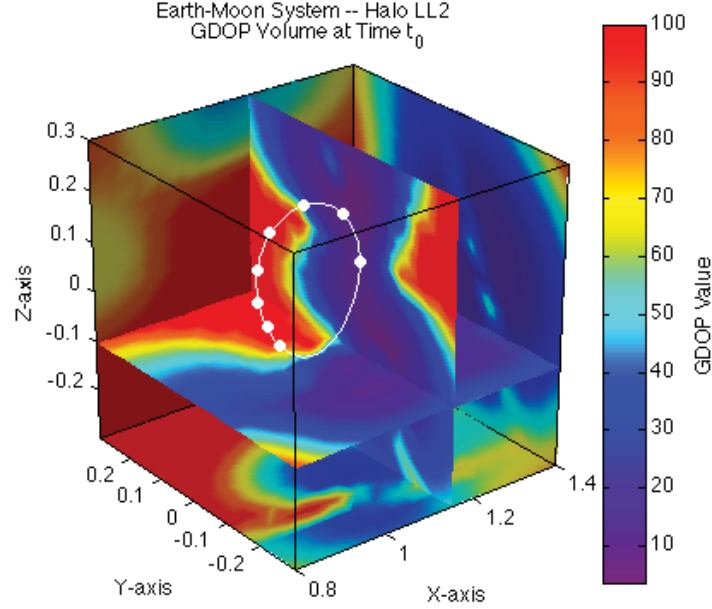
Figure 7: A volumetric plot of the GDOP values in a region about a representative LL2 halo orbit (indicated by the white line with the white dots showing the positions of 8 sample spacecraft) at a given point in time. The color scale is truncated to 100 to prevent outliers from washing out the details.

As shown in Fig.7, the asymmetric spacing of the spacecrafts illustrates how the better GDOP values will develop askew towards the regions favoring the most widespread view of said spacecrafts. The four dimensional integral for the depicted constellation is 87.5964.

OPTIMIZATION OVER THE SET OF PERIODIC ORBITS

Give the above metrics (generically denoted as J), one can then optimize over the set of periodic orbits, that is solve the following variation problem:

$$MaxJ(x_0(.)) \quad \text{subject to} \quad \begin{cases} \dot{x}_0 = \frac{1}{T}f(x_0, t) \text{ (dynamics constraints)} \\ x_0(t+1) = x_0(t) \text{ (periodic orbit condition)} \end{cases} \tag{15}$$

Here, the time has been normalized by the period T so that the periodic orbits $x_0(t)$ have a unit period. The vector field f represents the CR3BP dynamics.

As mentioned in the dynamical review section, the set of periodic orbits can be locally organized as a 1-dimensional curve (characteristic). In as much as our optimization metric do not depend on

13

the phase on the orbit, the above optimization problem is locally an optimization problem over a single real variable. Globally, the different periodic orbit branches intersect to form a bifurcation diagram, and the above optimization problem thus become optimization of a graph with 1-dimensional arcs.

Thus, in order to solve the above problem, one can simply evaluate the cost function J over the characteristic and determine the maximum value. One proceed exactly as for generating the bifurcation diagram shown in Figure 3 with the addition of the cost function evaluation along the way. Namely, starting from known solutions (here from the libration points LL1 and LL2), one continue each solution branch by branch, detecting bifurcation points. At the bifurcation points, cone continues the new branches and evaluate the value of the cost function. The resulting bifurcation diagram with colored coded by the variation in alpha parameter is shown in Figure 8.
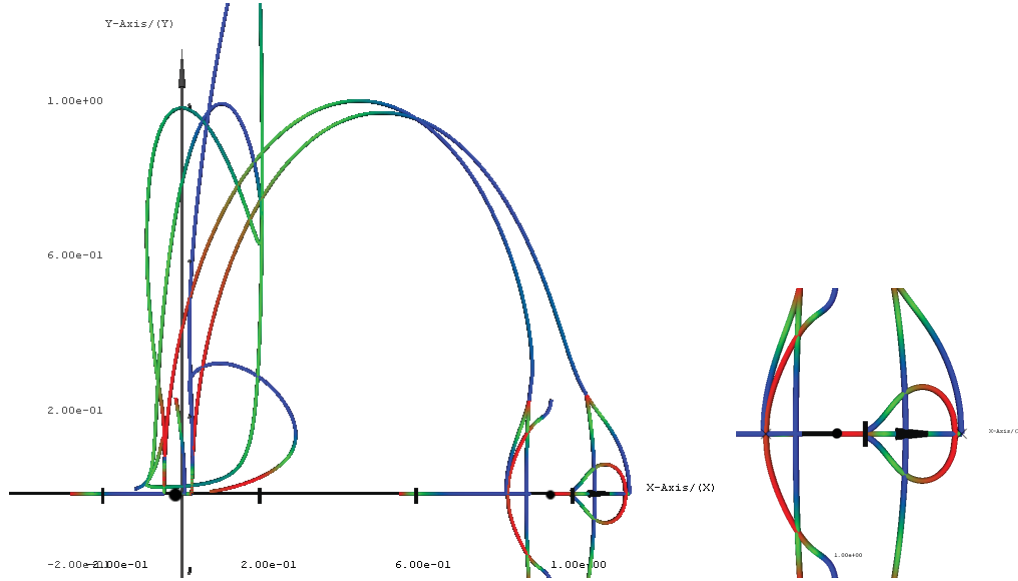
Figure 8: Bifurcation for the CR3BP, starting from the LL1 and LL2 points. The color along each branch corresponds to the period of the orbit, blue representing a shorter period and red a larger period. The black dots represent the location of the Earth and Moon. Left: global overview. Right: Zoom near the Moon.

As can be observed, the variation of α increases along the vertical families, corresponding to an increase in size of the orbits. For the Halo family, the cost function decreases with increase halo orbit size. While counter-intuitive at first, this phenomena is due to the domination of a single body (the Moon) as the halo orbits increase in size.

CONCLUSIONS

In this paper, we explored several families of periodic orbits cycling between the Earth and the Moon for a constellation of telecommunications and navigation beacons to support transport between the Earth and the Moon. To further enable the autonomous navigation of such a system, we extended the notion of relative navigation, LIAISON, introduced by Hill, Lo, and Born by using their α parameter to define a new metric for navigation, $Var(\alpha)$, which measures the bounded vari-

ation of α. Using this metric and the GDOP metric, we optimized the constellation design over several families of periodic orbits. This preliminary analysis will be continued in a series of future papers.

ACKNOWLEDGMENTS

REFERENCES

[1] Keric Hill and George H. Born. "Autonomous Interplanetary Orbit Determination Using Satellite-to-Satellite Tracking", *Journal of Guidance, Control, and Dynamics*, Vol. 30, No. 3, May - June 2007.

[2] Kathleen Connor Howell. "Three-Dimensional, Periodic, Halo-Orbits", *Celestial Mechanics*, Vol. 32, 1984, pp. 53-71.

[3] Victor Szebehely. *Theory of Orbits*, Academic Press, New York, 1967.

[4] Randy C. Paffenroth. "AUTO2000 Software", 2000.

[5] Hofmann-Wellenhof, B., Lichteneggar, H., and J. Collins. *GPS Theory and Practice*, 2nd Ed., Springer-Verlag, Wien, 1993.

[6] Tapley, B., Schutz, B., and G. Born. *Statistical Orbit Determination*, Elsevier, Burlington, MA, 2004.

[7] Erwin Kreyszig, *Advanced Engineering Mathematics*, 9th Ed., John Wiley & Sons, Inc., NY, 2006.

[8] Michael Athans, "The Matrix Minimum Principle", *Information and Control*, Vol.11, pp.592-608, 1968.

APPENDICES

This appendix provides further details about the derivations of the different navigation metrics referred to in the text.

Accuracy Measures for the End-User: The DOP Factors

The end-user is considered to be any spacecraft (that is not part of the constellation) that will be using the constellation for navigation purposes, mimicking GPS receiver/transmitter relationships. As such, the GPS metrics are used synonymously with the liaison constellation without any loss of generality.

The Dilution of Precision (DOP) factor is a metric often used in navigation systems as a way to gauge the accuracy of a solution. In this case, the solution specifically refers to the least-squares solution to the non-linear problem of determining an observer's position given only ranging measurements from multiple sources (i.e. satellites).

The formulation of this model starts with describing the position of an observer relative to a satellite in a chosen reference frame. This kinematic positioning is defined by a biased range quantity, aptly termed pseudorange. In its most basic form the pseudorange can be expressed as the sum of the geometric range between the observer and the satellite plus an error term. In some texts, this error term is explicitly attributed to a clock bias created from the observer and/or the satellites, but for this presentation, the error term is intentionally left ambiguous.

Note: the notation presented in this discussion is a modified combination of nomenclature used by Hofmann-Wellenhof et. al.[5] and Tapley et. al.[6]

$$R_{ij}(t) = \rho_{ij}(t) + \epsilon_{ij}(t) \tag{16}$$

The subscripts i and j, refer to the ith observer and the jth satellite, respectively. $R_{ij}(t)$ is the pseudorange (i.e. the actual scalar measurement provided by the satellite), $\rho_{ij}(t)$ is the geometric range of the observer with respect to the satellite, and $\epsilon_{ij}(t)$ is a generic error term.

It should be understood that all quantities are examined at some epoch t, and as such the explicit denotation of the functional dependencies on time will be omitted henceforth for reading clarity.

In order to write the Euclidean distance (range) in 3-dimensional coordinates, a reference frame and associated coordinate system must be chosen. In practice, since the satellite coordinates must be known *a priori*, a convenient coordinate system would be one where those coordinates are easily expressed. For the purposes of this generic illustration, the reference frame will be the neighborhood of the primary gravitational body and the rectangular, Cartesian coordinate system will be centered and fixed to the primary itself (i.e. the coordinate axes rotate with the primary). Now the range can be expressed as

$$\begin{aligned} \rho_{ij} &= \sqrt{(X_j - X_i)^2 + (Y_j - Y_i)^2 + (Z_j - Z_i)^2} \\ &\equiv f(X_i, Y_i, Z_i) \end{aligned} \tag{17}$$

where X_j, Y_j, Z_j are the known coordinates of satellite j and X_i, Y_i, Z_i are the unknown coordinates of observer i. Since the observer-satellite range is a non-linear function of the observer's position, an adjustment to the model is needed to find a solution for the system.

One technique is to replace the non-linear model with an approximated linearized version. A process is then applied by which an initial estimate is refined through successive iterations to reach a solution. This process is known as the non-linear least squares method.

The idea is to decompose the unknowns into a known part and an unknown part, or in other words, an estimated solution and a deviation. The estimated model can then be expanded via a Taylor series to approximate the function as an infinite sum of successive derivatives with respect to the state. If the reference solution is sufficiently close to the true solution, then the expansion can be truncated after the linear term. This omission of higher order terms is considered "linearization".

First, an approximated distance, analogous to the actual distance, can be defined as

$$
\begin{aligned}
\rho_{ij}^* &= \sqrt{(X_j - X_i^*)^2 + (Y_j - Y_i^*)^2 + (Z_j - Z_i^*)^2} \\
&\equiv f\left(X_i^*, Y_i^*, Z_i^*\right)
\end{aligned}
\tag{18}
$$

where the estimated model parameters are expressed in relation to the actual parameters as

$$
\begin{aligned}
X_i &= X_i^* + \Delta X_i \\
Y_i &= Y_i^* + \Delta Y_i \\
Z_i &= Z_i^* + \Delta Z_i
\end{aligned}
\tag{19}
$$

with X_i^*, Y_i^*, Z_i^* as the knowns (i.e. estimated parameters or initial guesses) and ΔX_i, ΔY_i, ΔZ_i as the new unknowns (i.e. deviations). Then substituting the parameter definitions from (19) into the range function given in (17) yields an equivalent expression that can then be expanded in a Taylor series as

$$
f\left(X_i, Y_i, Z_i\right) \equiv f\left(X_i^* + \Delta X_i, Y_i^* + \Delta Y_i, Z_i^* + \Delta Z_i\right) =
$$
$$
f\left(X_i^*, Y_i^*, Z_i^*\right) + \frac{\partial f\left(X_i^*, Y_i^*, Z_i^*\right)}{\partial X_i^*} \Delta X_i + \frac{\partial f\left(X_i^*, Y_i^*, Z_i^*\right)}{\partial Y_i^*} \Delta Y_i + \frac{\partial f\left(X_i^*, Y_i^*, Z_i^*\right)}{\partial Z_i^*} \Delta Z_i \quad \dots
\tag{20}
$$

where the expansion is truncated after the linear terms. The partials are computed by differentiating (18).

$$
\begin{aligned}
\frac{\partial f\left(X_i^*, Y_i^*, Z_i^*\right)}{\partial X_i^*} &= -\frac{X_j - X_i^*}{\rho_{ij}^*} \\
\frac{\partial f\left(X_i^*, Y_i^*, Z_i^*\right)}{\partial Y_i^*} &= -\frac{Y_j - Y_i^*}{\rho_{ij}^*} \\
\frac{\partial f\left(X_i^*, Y_i^*, Z_i^*\right)}{\partial Z_i^*} &= -\frac{Z_j - Z_i^*}{\rho_{ij}^*}
\end{aligned}
\tag{21}
$$

Putting everything together gives an expression for the range as a linear function of the new unknowns.

$$
\rho_{ij} = \rho_{ij}^* - \frac{X_j - X_i^*}{\rho_{ij}^*} \Delta X_i - \frac{Y_j - Y_i^*}{\rho_{ij}^*} \Delta Y_i - \frac{Z_j - Z_i^*}{\rho_{ij}^*} \Delta Z_i
\tag{22}
$$

Combining terms back into the original expression given by (16) yields the linear approximated model.

$$
R_{ij} = \rho_{ij}^* - \frac{X_j - X_i^*}{\rho_{ij}^*} \Delta X_i - \frac{Y_j - Y_i^*}{\rho_{ij}^*} \Delta Y_i - \frac{Z_j - Z_i^*}{\rho_{ij}^*} \Delta Z_i + \epsilon_{ij}
\tag{23}
$$

Rearranging terms by putting all of the knowns on the left-hand side of the equation and leaving the unknowns on the right-hand side gives

$$R_{ij} - \rho_{ij}^* = -\frac{X_j - X_i^*}{\rho_{ij}^*} \Delta X_i - \frac{Y_j - Y_i^*}{\rho_{ij}^*} \Delta Y_i - \frac{Z_j - Z_i^*}{\rho_{ij}^*} \Delta Z_i + \epsilon_{ij} \tag{24}$$

And to simplify the expression of the linear system, terms are grouped together into more convenient expressions. The observation residuals are defined as y_j and the partials of the mapping matrix as H_{XYZij}.

$$
\begin{aligned}
y_j &= R_{ij} - \rho_{ij}^* \\
H_{Xij} &= -\frac{X_j - X_i^*}{\rho_{ij}^*} \\
H_{Yij} &= -\frac{Y_j - Y_i^*}{\rho_{ij}^*} \\
H_{Zij} &= -\frac{Z_j - Z_i^*}{\rho_{ij}^*}
\end{aligned}
\tag{25}
$$

The equation for this model has four unknowns, namely ΔX_i, ΔY_i, ΔZ_i, and ϵ_{ij}. Conveniently, due to linear independence, a system of linear equations will arise from the addition of multiple observations. Since the minimum number of observations required to solve the linear system must match the number of unknowns, a system develops with four equations and four unknowns (where each of the equations is contributed by a different satellite).

$$
\begin{aligned}
y_1 &= H_{Xi1}\Delta X_i + H_{Yi1}\Delta Y_i + H_{Zi1}\Delta Z_i + \epsilon_{i1} \\
y_2 &= H_{Xi2}\Delta X_i + H_{Yi2}\Delta Y_i + H_{Zi2}\Delta Z_i + \epsilon_{i2} \\
y_3 &= H_{Xi3}\Delta X_i + H_{Yi3}\Delta Y_i + H_{Zi3}\Delta Z_i + \epsilon_{i3} \\
y_4 &= H_{Xi4}\Delta X_i + H_{Yi4}\Delta Y_i + H_{Zi4}\Delta Z_i + \epsilon_{i4}
\end{aligned}
\tag{26}
$$

Here a digression is instructive to explain the construction of the Jacobian.

$$
\mathbf{J} = \begin{bmatrix}
\frac{\partial y_1}{\partial \Delta X_i} & \frac{\partial y_1}{\partial \Delta Y_i} & \frac{\partial y_1}{\partial \Delta Z_i} & \frac{\partial y_1}{\partial \epsilon_{i1}} \\[2ex]
\frac{\partial y_2}{\partial \Delta X_i} & \frac{\partial y_2}{\partial \Delta Y_i} & \frac{\partial y_2}{\partial \Delta Z_i} & \frac{\partial y_2}{\partial \epsilon_{i2}} \\[2ex]
\frac{\partial y_3}{\partial \Delta X_i} & \frac{\partial y_3}{\partial \Delta Y_i} & \frac{\partial y_3}{\partial \Delta Z_i} & \frac{\partial y_3}{\partial \epsilon_{i3}} \\[2ex]
\frac{\partial y_4}{\partial \Delta X_i} & \frac{\partial y_4}{\partial \Delta Y_i} & \frac{\partial y_4}{\partial \Delta Z_i} & \frac{\partial y_4}{\partial \epsilon_{i4}}
\end{bmatrix}
\tag{27}
$$

It is important to distinguish that the traditional "mapping matrix" H, has been folded into a more generic Jacobian $\mathbf{J}$. This is seen by

$$H = \left[\frac{\partial \rho_{ij}}{\partial X, Y, Z}\right]_i^* = \frac{\partial y_j}{\partial \Delta X_i, \Delta Y_i, \Delta Z_i} \tag{28}$$

Including the unknown errors as part of the state deviation vector allows the expression of the Jacobian to contain both the mapping matrix and the error partials. Writing the Jacobian in this fashion also ensures the non-dimensionality of its values.

$$
\boldsymbol{y} = \begin{bmatrix} y_1 \\ y_2 \\ y_3 \\ y_4 \end{bmatrix} \qquad \mathbf{J} = \begin{bmatrix} H_{Xi1} & H_{Yi1} & H_{Zi1} & 1 \\ H_{Xi2} & H_{Yi2} & H_{Zi2} & 1 \\ H_{Xi3} & H_{Yi3} & H_{Zi3} & 1 \\ H_{Xi4} & H_{Yi4} & H_{Zi4} & 1 \end{bmatrix} \qquad \hat{\boldsymbol{x}} = \begin{bmatrix} \Delta X_i \\ \Delta Y_i \\ \Delta Z_i \\ \epsilon_i \end{bmatrix} \tag{29}
$$

The linear system may now be expressed in the form of a matrix equation.

$$
\boldsymbol{y} = \mathbf{J}\hat{\boldsymbol{x}} \tag{30}
$$

The well known solution to this linear system is

$$
\hat{\boldsymbol{x}} = \left(\mathbf{J}^T\mathbf{J}\right)^{-1}\mathbf{J}^T\boldsymbol{y} \tag{31}
$$

where the inverse of the information matrix, $\mathbf{J}^T\mathbf{J}$, is defined as the covariance matrix, P. Note that the information matrix must be non-singular in order to solve the system. In this formulation of the least-squares solution, the weighting matrix (not shown) is taken to be identity, as is the state transition matrix (also not shown).

Attention should now focus on the analysis of the covariance matrix. Identifying the terms explicitly,

$$
P = \left(\mathbf{J}^T\mathbf{J}\right)^{-1} = \begin{bmatrix} P_{XX} & P_{XY} & P_{XZ} & P_{Xt} \\ P_{XY} & P_{YY} & P_{YZ} & P_{Yt} \\ P_{XZ} & P_{YZ} & P_{ZZ} & P_{Zt} \\ P_{Xt} & P_{Yt} & P_{Zt} & P_{tt} \end{bmatrix} \tag{32}
$$

where the variances are located on the main diagonal of the matrix P. The variances can be expressed as the squares of the standard deviations, σ.

$$
\begin{array}{rcl}
P_{XX} & = & \sigma_X^2 \\
P_{YY} & = & \sigma_Y^2 \\
P_{ZZ} & = & \sigma_Z^2 \\
P_{tt} & = & \sigma_t^2
\end{array} \tag{33}
$$

The following five equations are the conventional definitions for the Dilution of Precision parameters:

$$
\begin{array}{rcl}
\text{GDOP} & = & \sqrt{\sigma_X^2 + \sigma_Y^2 + \sigma_Z^2 + \sigma_t^2} \\
\end{array} \tag{34}
$$

$$
\begin{array}{rcl}
\text{PDOP} & = & \sqrt{\sigma_X^2 + \sigma_Y^2 + \sigma_Z^2} \\
\end{array} \tag{35}
$$

$$
\begin{array}{rcl}
\text{TDOP} & = & \sqrt{\sigma_t^2} \\
\end{array} \tag{36}
$$

$$
\begin{array}{rcl}
\text{HDOP} & = & \sqrt{\sigma_X^2 + \sigma_Y^2} \\
\end{array} \tag{37}
$$

$$
\begin{array}{rcl}
\text{VDOP} & = & \sqrt{\sigma_Z^2} \\
\end{array} \tag{38}
$$

where the first letters preceding DOP stand for Geometric, Position, Time, Horizontal, and Vertical respectively. Recognize that the DOP parameters are related to each other in the following manner.

$$\text{GDOP}^2 = \text{PDOP}^2 + \text{TDOP}^2$$

$$\text{PDOP}^2 = \text{HDOP}^2 + \text{VDOP}^2$$

$$\text{GDOP}^2 = \text{HDOP}^2 + \text{VDOP}^2 + \text{TDOP}^2$$

Although numerically derived from a common statistical error measure, operationally, DOP is a term used almost exclusively for values that arise in particular from the 4×4 covariance matrix of the aforementioned system.

Recall that the DOP parameters described above are relative to a primary body-centered and -fixed coordinate system. The horizontal and vertical components are, likewise, relative to the coordinate system used to compute them. A transformation may be necessary to relate the centered/fixed system to the local coordinate system (if it is desired to explicitly define the precisions relative to the observer). This rotation, or similarity transformation, is fairly straightforward and may be expressed as

$$Q_{\text{local}} = RQR^T \tag{39}$$

where R is any rotation matrix that relates the initial coordinate system to one that is local to the observer and Q is a sub-matrix of P, with elements defined as

$$Q = \begin{bmatrix} P_{XX} & P_{XY} & P_{XZ} \\ P_{XY} & P_{YY} & P_{YZ} \\ P_{XZ} & P_{YZ} & P_{ZZ} \end{bmatrix} \tag{40}$$

Note that only after a transformation to a local coordinate system, will the HDOP and VDOP values hold meaning for the observer. GDOP will remain unaffected from the rotation since the trace of a square matrix is invariant under similarity transformations.

For further insight it is useful to consider a geometric interpretation of DOP. Notice that the first three columns of the Jacobian provide the components of the unit vectors ($\Delta\rho$) that point from the satellites to the best estimate of the observer. These unit vectors define the vertices of a polyhedral surface. For example, using the four satellites posed in this discussion, the surface is a tetrahedron.

$$\begin{aligned} \Delta\boldsymbol{\rho}_{i1} &= (J_{11}, J_{12}, J_{13}) \\ \Delta\boldsymbol{\rho}_{i2} &= (J_{21}, J_{22}, J_{23}) \\ \Delta\boldsymbol{\rho}_{i3} &= (J_{31}, J_{32}, J_{33}) \\ \Delta\boldsymbol{\rho}_{i4} &= (J_{41}, J_{42}, J_{43}) \end{aligned} \tag{41}$$

The largest theoretical volume achievable with such a structure is attained by a "regular" polyhedron, where each face is an equal-sided polygon. Considering the special case of the tetrahedron formed above, the surface is constructed with the observer at the origin of a temporary coordinate system, one vertex at the zenith, and the other three vertices equally separated azimuthally ($120°$ apart) at an elevation of $-19.471°$ (resulting from $\pi/2 - \cos^{-1}(-1/3)$) relative to the horizon plane.
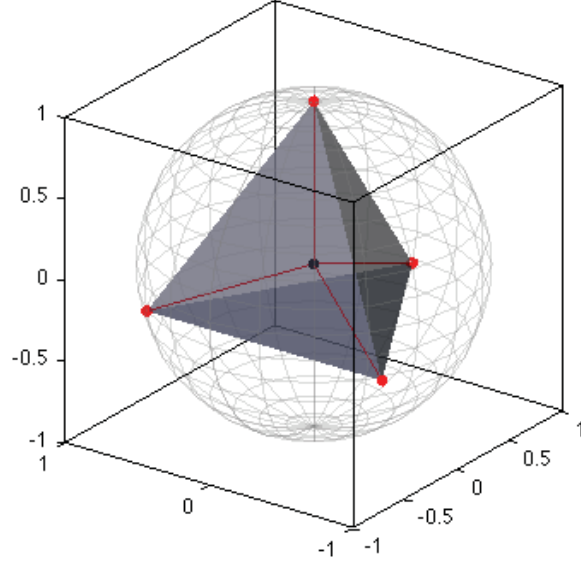
Figure 9: A regular tetrahedron is the theoretical maximum structure formed when using four points (i.e. satellites); one at the zenith and the other three equally spaced azimuthally at an elevation of $-19.471°$, with the observer at the origin; shown here circumscribed by a unit sphere.

Taking the scalar triple product of any three edges that intersect at a common vertex will yield the volume of the parallelepiped described by those vectors. This value turns out to be directly proportional to the determinant of the Jacobian.

Scalar Triple Product: $[A, B, C] = A \cdot (B \times C)$

$$
\begin{aligned}
\left[(\Delta\boldsymbol{\rho}_{i4} - \Delta\boldsymbol{\rho}_{i1}), (\Delta\boldsymbol{\rho}_{i3} - \Delta\boldsymbol{\rho}_{i1}), (\Delta\boldsymbol{\rho}_{i2} - \Delta\boldsymbol{\rho}_{i1})\right] &= -3.079 \\
\left[(\Delta\boldsymbol{\rho}_{i1} - \Delta\boldsymbol{\rho}_{i2}), (\Delta\boldsymbol{\rho}_{i4} - \Delta\boldsymbol{\rho}_{i2}), (\Delta\boldsymbol{\rho}_{i3} - \Delta\boldsymbol{\rho}_{i2})\right] &= 3.079 \\
\left[(\Delta\boldsymbol{\rho}_{i2} - \Delta\boldsymbol{\rho}_{i3}), (\Delta\boldsymbol{\rho}_{i1} - \Delta\boldsymbol{\rho}_{i3}), (\Delta\boldsymbol{\rho}_{i4} - \Delta\boldsymbol{\rho}_{i3})\right] &= -3.079 \\
\left[(\Delta\boldsymbol{\rho}_{i3} - \Delta\boldsymbol{\rho}_{i4}), (\Delta\boldsymbol{\rho}_{i2} - \Delta\boldsymbol{\rho}_{i4}), (\Delta\boldsymbol{\rho}_{i1} - \Delta\boldsymbol{\rho}_{i4})\right] &= 3.079
\end{aligned}
\tag{42}
$$

where the sign is affected by the ordering of the vertices (shown here as a simple cyclic permutation of indices). The determinant of the Jacobian, however, is constant.

$$
\det\left(\mathbf{J}\right) = -3.079 \tag{43}
$$

Given this maximal structure, the corresponding theoretical minimums for the DOP values are

21

computed from equations (34)-(38)

$$
\begin{aligned}
\text{GDOP} &= 1.581 \\
\text{PDOP} &= 1.500 \\
\text{TDOP} &= 0.500 \\
\text{HDOP} &= 1.225 \\
\text{VDOP} &= 0.866
\end{aligned}
$$

The insight gained from the geometrical abstraction of the Jacobian, is that "good" spacecraft geometries mirror "low" DOP values. In other words, to achieve better measurement accuracy, the ideal placement of satellites relative to the observer should be widespread in the sky with large angular separations between them.

Optimizing Spacecraft Configuration within a Constellation: The β Parameter

The orbit determination problem is inherently non-linear. As such, the problem needs to be linearized, whereby the non-linear model is approximated by a Taylor series expansion that is truncated after the linear term. Only after this is accomplished, can the method of least-squares be applied to solve the system.

The first step is to define the state vector. Since the unknown states of two spacecrafts are desired, the state vector of the system should naturally contain the position and velocity elements for both spacecraft (designated with subscripts 1 and 2). This is described in rectangular Cartesian coordinates as

$$
\boldsymbol{X}_i = [x_1 \quad y_1 \quad z_1 \quad \dot{x}_1 \quad \dot{y}_1 \quad \dot{z}_1 \quad x_2 \quad y_2 \quad z_2 \quad \dot{x}_2 \quad \dot{y}_2 \quad \dot{z}_2]_i^T \tag{44}
$$

where $\boldsymbol{X}_i$ will be used as short-hand for writing the state as a function of time $\boldsymbol{X}(t_i)$. Each original unknown is decomposed into an estimated solution and a deviation. Hence,

$$
\begin{aligned}
x_k &= x_k^* + \Delta x_k \\
y_k &= y_k^* + \Delta y_k \\
z_k &= z_k^* + \Delta z_k \\
\dot{x}_k &= \dot{x}_k^* + \Delta \dot{x}_k \\
\dot{y}_k &= \dot{y}_k^* + \Delta \dot{y}_k \\
\dot{z}_k &= \dot{z}_k^* + \Delta \dot{z}_k
\end{aligned} \tag{45}
$$

for the spacecraft index $k = 1, 2$, where the superscript $*$ indicates *a priori* estimated parameters and the Δ denotes deviations (all of which are implicitly functions of time). This modification allows for the expansion of the model about a reference trajectory, while maintaining a solution vector of deviations over which to minimize. Once the changes in the deviations no longer appreciably affect the nominal trajectory, then the process is said to have converged on the best estimate of the state. The reference trajectory and state deviation vector are defined, respectively, as

$$
\boldsymbol{X}_i^* = [x_1^* \quad y_1^* \quad z_1^* \quad \dot{x}_1^* \quad \dot{y}_1^* \quad \dot{z}_1^* \quad x_2^* \quad y_2^* \quad z_2^* \quad \dot{x}_2^* \quad \dot{y}_2^* \quad \dot{z}_2^*]_i^T \tag{46}
$$

$$
\boldsymbol{\Delta x}_i = [\Delta x_1 \ \Delta y_1 \ \Delta z_1 \ \Delta \dot{x}_1 \ \Delta \dot{y}_1 \ \Delta \dot{z}_1 \ \Delta x_2 \ \Delta y_2 \ \Delta z_2 \ \Delta \dot{x}_2 \ \Delta \dot{y}_2 \ \Delta \dot{z}_2]_i^T \tag{47}
$$

22

From the observability standpoint, in order for the solution to be uniquely determined, it is necessary to relate the measurements to the set of unknowns. The observation-state mapping matrix shows how computed observations vary with respect to the best estimate of the state (i.e. reference trajectory) and is defined as

$$\tilde{H}_i = \left[\frac{\partial G}{\partial \boldsymbol{X}} \right]_i^* \tag{48}$$

where G is a function that computes observations given the estimate of the state, $\boldsymbol{X}_i^*$, at a particular epoch, t_i. The subscript i is used to index into the data span. For liaison navigation, the observation type is range, and therefore, the generating function takes the form

$$G\left(\boldsymbol{X}_i^*, t_i\right) = \rho_i^* \tag{49}$$

$$\rho_i^* = \left[\sqrt{(x_2 - x_1)^2 + (y_2 - y_1)^2 + (z_2 - z_1)^2} \right]_i^* \tag{50}$$

where ρ_i^* is the computed range. The Euclidean distance is a non-linear function of the state variables. The observation-state mapping matrix can now be more explicitly written as

$$\tilde{H}_i = \left[\begin{array}{cccccccccccc} \frac{\partial \rho}{\partial x_1} & \frac{\partial \rho}{\partial y_1} & \frac{\partial \rho}{\partial z_1} & \frac{\partial \rho}{\partial \dot{x}_1} & \frac{\partial \rho}{\partial \dot{y}_1} & \frac{\partial \rho}{\partial \dot{z}_1} & \frac{\partial \rho}{\partial x_2} & \frac{\partial \rho}{\partial y_2} & \frac{\partial \rho}{\partial z_2} & \frac{\partial \rho}{\partial \dot{x}_2} & \frac{\partial \rho}{\partial \dot{y}_2} & \frac{\partial \rho}{\partial \dot{z}_2} \end{array} \right]_i^* \tag{51}$$

In a perfect situation, the observation generating function should identically yield the actual observations made from the spacecraft. More generically, however, the observations can be assumed to follow the form

$$\boldsymbol{Y}_i = G\left(\boldsymbol{X}_i^*, t_i\right) + \boldsymbol{\epsilon}_i \tag{52}$$

where $\boldsymbol{Y}_i$ are the observations themselves and $\boldsymbol{\epsilon}_i$ are the errors associated with those measurements. This last term should capture any observational errors but may also help to reveal any systematic modeling errors. The $\tilde{H}_i$ matrix at time t_i may be mapped back to the initial epoch t_0 using the state transition matrix.

$$H_i = \tilde{H}_i \, \Phi(t_i, t_0) \tag{53}$$

where $\Phi(t_i, t_0)$ is the state transition matrix from the initial epoch t_0 to some later time t_i. The construction of the state transition matrix is provided later in this section. This reverse mapping will allow many observations at disparate times to be related back to a common epoch where the least-squares evaluation will take place. The total mapping matrix H_i is accumulated by appending every $\tilde{H}_i$ that is computed

$$H \equiv \left[\begin{array}{c} H_1 \\ \vdots \\ H_\ell \end{array} \right] \tag{54}$$

for ℓ total observations. Note that the system remains solvable if and only if the total number of observations is equal to or greater than the number of unknowns (i.e. components in the state deviation vector). Operationally, this lower limit tends not to be an issue due to the number of observations often far exceeding the number of unknowns, otherwise known as an overdetermined system. By way of processing all of the information over a given observation interval in a single run, this particular least-squares application has earned the title, batch least-squares solution, or simply, batch processor.

The batch least-squares solution has several known short-comings. In an effort to mitigate some of these deficiencies, a slightly modified approach is favored which accounts for additional weighting information. This method is not surprisingly called the weighted batch least-squares solution.

The novelty of this improved method is in its usage of a weighting matrix, where *a priori* information may be incorporated to control the influence of certain observations over others. The resulting augmentation to the normal matrix is so-called the information matrix

$$\Lambda = H^T W H = \sum_{j=1}^{\ell} H_j^T W H_j \tag{55}$$

where ℓ observations are accumulated in a summation to form the total information matrix Λ. Supposing that the mapping and weighting matrices are comprised of real entries, the information matrix will be positive definite by construction. Perhaps the most familiar form of this quantity is its inverse, otherwise known as the variance-covariance matrix (often abbreviated to just covariance matrix).

$$P \equiv \Lambda^{-1} = (H^T W H)^{-1} \tag{56}$$

Recall that the covariance matrix computed thus far is only for one instant in time, namely the initial epoch t_0. In order to investigate the time evolution of the covariance matrix, it must be propagated forward in time by means of a similarity transformation involving the state transition matrix.

Because the covariance matrix is used to compute the variances of errors in the state parameters and the correlations between these errors, it can ultimately be used to compute orbit determination (navigation knowledge) metrics. To compare the accuracy of orbit estimates, the batch covariance is propagated over the entire data span as

$$P_i = \Phi(t_i, t_0) \, P_0 \, \Phi^T(t_i, t_0) \tag{57}$$

Here, a digression is instructive to explain the construction of the state transition matrix. $\Phi(t_i, t_0)$ maps the state deviation (relative to the reference trajectory) from the observation epoch t_0 to some later epoch t_i. The state transition matrix is computed from partial derivatives as $\Phi(t_i, t_0) = \partial \boldsymbol{X} / \partial \boldsymbol{X}_0$. However, instead of differentiation, the state transition matrix can be computed by numerically integrating the variational equations

$$\dot{\Phi}(t_i, t_0) = A(t_i)\Phi(t_i, t_0), \qquad \text{with} \ \ \Phi(t_0, t_0) = I \tag{58}$$

where the forcing function, $A(t_i)$, captures the linearized dynamics of the system in the form of

$$A(t_i) = \left[\frac{\partial \boldsymbol{F}(\boldsymbol{X}, t)}{\partial \boldsymbol{X}} \right]_i^* \tag{59}$$

with $\dot{\boldsymbol{X}}^* = \boldsymbol{F}(\boldsymbol{X}_i^*, t_i)$ and initial conditions $\boldsymbol{X}_0^*$, evaluated on the reference (baseline or nominal) trajectory. A formulation of this forcing function as it pertains to the dynamical system for liaison navigation is briefly presented. Consider the circular restricted three-body problem for one spacecraft, with three degrees of freedom generically written as

$$\begin{aligned}
\ddot{x}_1 &= F_1(x_1, \, x_2, \, x_3, \, \dot{x}_1, \, \dot{x}_2, \, \dot{x}_3) \\
\ddot{x}_2 &= F_2(x_1, \, x_2, \, x_3, \, \dot{x}_1, \, \dot{x}_2, \, \dot{x}_3) \\
\ddot{x}_3 &= F_3(x_1, \, x_2, \, x_3, \, \dot{x}_1, \, \dot{x}_2, \, \dot{x}_3)
\end{aligned} \tag{60}$$

Expressing this system of second order differential equations as a system of coupled first order differential equations yields

$$
\begin{aligned}
\dot{x}_1 &= x_4 \\
\dot{x}_2 &= x_5 \\
\dot{x}_3 &= x_6 \\
\dot{x}_4 &= F_1(x_1,\, x_2,\, x_3,\, x_4,\, x_5,\, x_6) \\
\dot{x}_5 &= F_2(x_1,\, x_2,\, x_3,\, x_4,\, x_5,\, x_6) \\
\dot{x}_6 &= F_3(x_1,\, x_2,\, x_3,\, x_4,\, x_5,\, x_6)
\end{aligned}
\tag{61}
$$

Thus, the forcing function, $A(t_i)$, is the partials of these first order differential equations of motion with respect to the state. Since delving into the details of this function detracts from the scope of this section, no further comment is given on the development of this function.

Returning to the error analysis, the information from the covariance matrix is used to generate the probability ellipsoid from which the orbit determination metric is computed. To generate this probability ellipsoid, we introduce the following theorem (Kreyszig[7]).

> *Theorem*: If $\hat{\mathbf{u}}_1$, $\hat{\mathbf{u}}_2$, $\ldots \hat{\mathbf{u}}_n$ is an orthonormal system of eigenvectors associated, respectively, with the eigenvalues λ_1, λ_2, $\ldots \lambda_n$ of an $n \times n$ symmetric positive definite matrix, P, and if $U = [\hat{\mathbf{u}}_1,\, \hat{\mathbf{u}}_2,\, \ldots \hat{\mathbf{u}}_n]_{n \times n}$, then $P' \equiv U^T P U = \text{diag}\,[\lambda_1,\, \lambda_2,\, \ldots \lambda_n]$, which is a diagonal matrix containing the eigenvalues of P.

The normalized eigenvectors $\hat{\mathbf{u}}_1$, $\hat{\mathbf{u}}_2$, $\ldots \hat{\mathbf{u}}_n$ are the principal axes of P and U^T is called the principal axes transformation (a.k.a. the modal matrix). Then $P' = \text{diag}\,[\lambda_1,\, \lambda_2,\, \ldots \lambda_n]$ is the covariance matrix associated with the principal axes. Consider the simplified case (Tapley et. al.[6]) where the estimation error vector can be represented as

$$
\Delta \boldsymbol{x} \equiv \boldsymbol{X} - \boldsymbol{X}^* \equiv [\tilde{x}\ \tilde{y}\ \tilde{z}]^T
\tag{62}
$$

with zero mean and covariance given by

$$
P = E\left[\Delta \boldsymbol{x} \Delta \boldsymbol{x}^T\right]
\tag{63}
$$

Note that, although unnecessary, the simplification of using only the position coordinates of $\Delta \boldsymbol{x}$, is illustrative in visualizing the ellipsoid in 3D. Accordingly, if the associated 3×3 portion of the estimation error covariance matrix is $[P]_{3 \times 3}$, then the equation for the probability ellipsoid is

$$
[\tilde{x}\ \tilde{y}\ \tilde{z}]\ [P]_{3 \times 3}^{-1}
\begin{bmatrix}
\tilde{x} \\
\tilde{y} \\
\tilde{z}
\end{bmatrix}
= \ell^2
\tag{64}
$$

which for $\ell = 3$, gives the 3σ error ellipsoid. The utility of the Central Limit Theorem for OD is that it gives assurance that observation errors in tracking systems, a sum of several random variables, tend to be normally (Gaussian) distributed. Therefore, assuming the combination of observation errors satisfy a trivariate Gaussian density function, the probability of the state estimation error falling inside this ellipsoid is 0.971.

From the formulation above, the length of the largest axis of the 3σ ellipsoid at epoch t_i, can be shown to be

$$\beta_i = 3 \max\left(\sqrt{\lambda_j}\right) \qquad \text{for } j = 1, 2, 3 \tag{65}$$

where λ_j are the eigenvalues of the submatrix $[P]_{3\times3}$. Following Hill and Born's description, several sequential developments of this metric can be defined to encompass various constellation configurations to indicate an overall sense of navigation accuracy.

Navigation Metric on the Class of Periodic Orbits: The $Var(\alpha)$ Parameter

The acceleration field of the Earth-Moon system is largely dominated by the presence of the two primary celestial bodies. While including additional perturbations, such as the third-body effect of the Sun or non-spherical effects of the Earth, may make the model more realistic, subsequent averaging techniques will negate the benefit of such high precision. So, the perturbed equations of motion for a spacecraft in this neighborhood may be simplified to include only the gravitational contributions of the Earth and Moon. Listed separately, the accelerations felt by a spacecraft due to the Earth and Moon, respectively, are

$$\ddot{\boldsymbol{r}}_{\text{Earth}} = -\mu_{\text{Earth}} \frac{\boldsymbol{r}}{r^3} \tag{66}$$

$$\ddot{\boldsymbol{r}}_{\text{Moon}} = -\mu_{\text{Moon}} \frac{\boldsymbol{\rho}}{\rho^3} \tag{67}$$

where the μ's are the gravitational parameters, $\boldsymbol{r}$ is the position vector to the spacecraft relative to the center of Earth, and $\boldsymbol{\rho}$ is the position vector from the spacecraft to the Moon. The unbolded versions of each of these vectors represents their magnitudes. Note that all position vectors, and consequently α, are implicit functions of (x, y, z) and time. Using these definitions, the strength of the acceleration, contributed by the Moon, compared to the total acceleration of the system may be computed as

$$
\begin{aligned}
\alpha_{\text{Moon}} &= \frac{|\ddot{\boldsymbol{r}}_{\text{Moon}}|}{|\ddot{\boldsymbol{r}}_{\text{Earth}}| + |\ddot{\boldsymbol{r}}_{\text{Moon}}|} \\[2ex]
&= \frac{\left|\mu_{\text{Moon}} \frac{\boldsymbol{\rho}}{\rho^3}\right|}{\left|\mu_{\text{Earth}} \frac{\boldsymbol{r}}{r^3}\right| + \left|\mu_{\text{Moon}} \frac{\boldsymbol{\rho}}{\rho^3}\right|}
\end{aligned}
\tag{68}
$$

For the remainder of this presentation, the subscript Moon, will be dropped from the α_{Moon} term for reading clarity.

As was discovered by Hill and Born, spacecrafts that are heavily influenced by both primaries are better suited for liaison navigation. α provides a way to determine the strength of the asymmetry felt by each spacecraft individually. However, in order to globally quantify the level of asymmetry experienced by an entire constellation, a new metric needs to be introduced.

Just as one can visually identify orbits that span large regions of asymmetry by comparing the orbits to the α map of a system, a mathematical analogy is constructed by computing the variations of the total derivative of α over one orbital period. Writing out Eq.(68) explicitly yields

$$\alpha = \left[1 + \bar{\mu} \frac{\rho^2}{r^2}\right]^{-1} \tag{69}$$

where $\bar{\mu}$ is the ratio of the gravitational parameters of the Earth and Moon, respectively. Since the total time derivative is quite lengthy, a method of successive substitutions is adopted to better show the relation.

$$\left| \frac{\mathrm{d}\alpha}{\mathrm{d}t} \right| = \left| -\alpha^2 \bar{\mu} \left[\frac{r^2 \frac{\mathrm{d}}{\mathrm{d}t}\left(\rho^2\right) - \rho^2 \frac{\mathrm{d}}{\mathrm{d}t}\left(r^2\right)}{r^4} \right] \right| \tag{70}$$

where the intermediate time derivatives are

$$\frac{\mathrm{d}}{\mathrm{d}t}\left(\rho^2\right) = 2\left[(x_m - x)(\dot{x}_m - \dot{x}) + (y_m - y)(\dot{y}_m - \dot{y}) + (z_m - z)(\dot{z}_m - \dot{z})\right] \tag{71}$$

$$\frac{\mathrm{d}}{\mathrm{d}t}\left(r^2\right) = 2\left(x\dot{x} + y\dot{y} + z\dot{z}\right) \tag{72}$$

where the "$\cdot$" indicates time derivative, and with the vector magnitudes defined as

$$\rho = \sqrt{(x_m - x)^2 + (y_m - y)^2 + (z_m - z)^2} \tag{73}$$

$$r = \sqrt{x^2 + y^2 + z^2} \tag{74}$$

Note that in this formulation, the entire 6-state vector is utilized to compute the variation of α. The integration of the absolute magnitude of the time variation of α now provides the global means to characterize an orbits span of asymmetry.